Open Access Library Journal
2022, Volume 9, e9086
ISSN Online: 2333-9721
ISSN Print: 2333-9705

Evidence of a Dark Matter that Is Not an Exotic Matter: WLM's Case

Stéphane Le Corre

Ecole Polytechnique Fédérale de Lausanne, Route Cantonale, Lausanne, Switzerland
Email: le.corre.stephane@hotmail.fr

How to cite this paper: Le Corre, S. (2022) Evidence of a Dark Matter that Is Not an Exotic Matter: WLM's Case. *Open Access Library Journal*, **9**: e9086.
https://doi.org/10.4236/oalib.1109086

Received: July 7, 2022
Accepted: August 23, 2022
Published: August 26, 2022

Abstract

A recent article reports new observations of the gaseous content of Wolf-Lundmark-Melotte (WLM), an archetype of isolated, gas-rich field dwarf galaxies in the Local Universe, which presents an unexpected situation, four trailing, extended gas clouds lying in the direction opposite to WLM's spatial motion, as well as a spatial offset between the WLM gas and stars, which rules out the near-completion merger hypothesis and suggests a process called ram-pressure stripping. For these authors, this finding could indicate either the presence of an intergalactic, gaseous reservoir far from large galaxies whose evolutionary role in galaxies, both large and small, may not be fully appreciated or the WLM galaxy is deficient in dark matter (DM). Here, we propose an explanation for which WLM galaxy is effectively deficient in DM and which allows explaining DM in the General Relativity Frame without an exotic matter. It explains the existence of gas clouds lying in the direction opposite to WLM's spatial motion, the number of four of these clouds, their location and the two bridges. Furthermore, this solution can explain the warping of WLM and the vertical position of WLM. This explanation also implies a slight shift and counterclockwise rotation of these clouds (unexplained by Ram pressure effect) and that the left (western) side of WLM is frontward. This explanation allows retrieving the density of the gaseous intergalactic medium and interstellar gaseous medium thanks to DM.

Subject Areas

Astrophysics, Dynamical System, Particle Physics

Keywords

Dark Matter, Galaxies, Dwarf-Local Group-Galaxies, ISM-Galaxies, Irregular-Galaxies, Kinematics and Dynamics-Intergalactic Medium

1. Introduction

In a recent article (Yanbin Yang *et al*., 2022) [1], Wolf-Lundmark-Melotte (WLM), an archetype of isolated, gas-rich field dwarf galaxies in the Local Universe presents an unexpected situation:

1) four trailing, extended gas clouds

2) lying in the direction opposite to WLM's spatial motion (due to Ram pressure)

3) with two bridges between WLM and two of the four clouds

We are going to explain this physical situation with a new explanation of dark matter (DM), without exotic matter or MOND theory, but simply with General Relativity (GR). This solution will be enough accurate to allow detecting and explaining two other characteristics of these clouds that can't be explained by Ram pressure:

4) a slight shift of the four clouds below the line of WLM's proper motion

5) a slight counterclockwise rotation of these clouds.

A previous article (Kepley *et al.* 2007) [2] also demonstrates an asymmetric field of WLM's velocity with its approaching (northern) and receding (southern) sides showing different rotational velocities and particularly:

6) its approaching side appears to be warped

7) a steeper velocity gradient for the approaching side than for the receding side in the inner region of the galaxy.

This explanation of dark matter will also explain this warping. In fact, several predictions of this DM's solution (Le Corre, 2015) [3], confirmed by observations, are used to explain WLM's case: existence of privileged alignments in a cluster, warping of galaxies and quantity of DM (*i.e.* orientation and value of the vector explaining DM). It will be deduced from these characteristics:

8) the left (western) side of WLM is frontward and the right (eastern) side is backward

9) the roughly vertical position of WLM is expected

10) the orientation of the vector explaining DM is close to the galactic plane of Milky Way (MW) in an interval of around ±20˚

11) the origin of the vector explaining DM is coming from galaxies' clusters.

And at the margin of this study, one will also notice that this dark matter explanation implies the warping of Milky Way (MW) and a higher than expected precession of this warping (recently observed).

But furthermore, certainly the main and more exciting results, this explanation of dark matter applied in the WLM's situation will allow retrieving:

12) the right quantity of DM (the good order of magnitude of the vector explaining DM)

13) the densities of interstellar gaseous medium (ISM) and gaseous intergalactic medium (IGM).

One writes "more exciting" because this explanation finally goes beyond the simple explanation of the specific case of WLM, it makes this potential solution

of dark matter (one of today's major physical problems) incredibly consistent and therefore relevant.

For this explanation, the previous points (1), (4), (6), (9), (10), (11), and (12) are a direct effect of DM. (8) and (13) are deduced indirectly thanks to DM solution. (2), (3), (5), and (7) are due to conventionally known physics.

2. Dark Matter as the 2nd Component of Gravitational Field of GR Generated by the Galaxies' Clusters (without Exotic Matter)

Before starting studying Wolf-Lundmark-Melotte galaxy (WLM), we remind briefly how General Relativity (GR) can explain dark matter (DM) as presented in (Le Corre, 2015) [3] to be able to use DM's idealization to the WLM's case.

2.1. Linearized General Relativity (GRL)

When we measure the rotational velocity at the end of the galaxies, we are far enough of the galaxies' center to consider that its own gravitational field in this distant area is very weak. Furthermore, for isolated dwarf galaxies (as WLM), gravitational influence of host galaxies is also very weak. Galaxies at the edge of clusters (once again as WLM), will also undergo very weak gravitational influence of the cluster (compared to the inner of the cluster). This last remark is to take in account because in this explanation, dark matter is not an exotic matter but the gravitational effect of the 2nd component of GR of the galaxies' clusters. For all these reasons, using the linearized equations of the GR in weak field (GRL) is justified. The advantage of GRL is to allow an easy understanding of several unusual gravitational effects (that we are going to use in this study). And above all, it allows taking advantage of the knowledge of electromagnetism (EM) because GRL equations leads to an idealization similar to EM equations (for example the existence of a field at large scale compare to the particle source as for a magnet).

We can find the linearisation of GR in (Hobson *et al.*, 2009) [4] or (Mashhoon, 2008) [5] for example. In this article, we will take the equivalent definitions of GR in weak gravitational field used in (Le Corre, 2015) [3]. It yields to the field equations (written as Poisson equations):

$$\Delta\varphi = 4\pi G\rho;\ \ \Delta H^i = \frac{4\pi G}{c^2}\rho u^i = 4\pi K^{-1}\rho u^i \tag{1}$$

With φ the traditional gravitational scalar potential, H^i a gravitational vector potential (specific to GR and generating the observed Lense-Thirring effect) and K a new constant defined by:

$$GK = c^2 \tag{2}$$

This definition gives $K^{-1} \sim 7.4\times10^{-28}$ (very small in magnitude compare to G).

With the following definitions of $\boldsymbol{g}$ (gravity field) and $\boldsymbol{k}$ (which we will name "gravitic field"), those relations can be obtained from the following equa-

tions (also called gravitomagnetism because of its proximity with EM):

$$\begin{aligned} &\boldsymbol{g} = -\boldsymbol{grad}\,\varphi;\ \ \boldsymbol{k} = \boldsymbol{rot}\,\boldsymbol{H} \\ &\boldsymbol{rot}\,\boldsymbol{g} = 0;\ \ div\boldsymbol{k} = 0; \\ &div\,\boldsymbol{g} = -4\pi G\rho;\ \ \boldsymbol{rot}\,\boldsymbol{k} = -4\pi K^{-1}\boldsymbol{j}_p \end{aligned} \tag{3}$$

The equations of geodesics in the linear approximation give the following movement equations:

$$\frac{\mathrm{d}^2\boldsymbol{x}}{\mathrm{d}t^2} \sim -\boldsymbol{grad}\,\varphi + 4\boldsymbol{v}\wedge\left(\boldsymbol{rot}\,\boldsymbol{H}\right) = \boldsymbol{g} + 4\boldsymbol{v}\wedge\boldsymbol{k}$$

2.2. General Relativity Explaining Dark Matter

The 2nd component of GRL (*i.e.* the term $4\boldsymbol{v}\wedge\boldsymbol{k}$) is at the origin of the Lense-Thirring effect observed and verified by several experiments, NASA's LAGEOS satellites or Gravity Probe B (Adler 2015) [6]. In this explanation of dark matter, instead of an exotic matter, one assumes that galaxies' clusters generate a gravitic field, $\boldsymbol{k}_0$, which embeds galaxies. Galaxies' velocities at their ends can be obtained as the equilibrium of the 3 forces (centrifugal force $\boldsymbol{F}_c$, gravitational force $\boldsymbol{F}_g$ due to $\boldsymbol{g}$ and the gravitational force $\boldsymbol{F}_k$ due to the environment gravitic field $\boldsymbol{k}_0$) as in **Figure 1**. It has been demonstrated that the own gravitic field of the galaxy is negligible at its ends (Letelier, 2006) [7], (Clifford M. Will, 2014) [8], (Bruni *et al.*, 2013) [9], (Le Corre, 2015) [3]:

In (Le Corre, 2015) [3], it is demonstrated from this equilibrium that an external field $\boldsymbol{k}_0$ can explain the rotational velocities of the galaxies with values in the interval $10^{-16.62} < k_0 < 10^{-16.3}$ (with unit of measurement s^{-1}). These values will be used further to retrieve the density ratio between IGM and ISM at the extremities of WLM.

Remark: As indicated in (Le Corre, 2015) [3], these values explain why the gravitic field (the dark matter) is imperceptible on Earth and its expression explains why it becomes detectable only on large structure (large r or large v). At this step, one can note the remarkable self-consistency of this "dark matter" explanation compare to the traditional assumption of an exotic matter (which would represent more than 5 times the baryonic matter in which we were embedded and that would be locally undetectable and furthermore of no need in our local physic equations). Furthermore, the gravitic field has all the expected qualities of dark

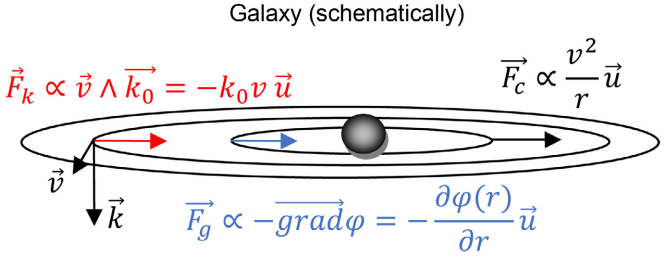

Figure 1. Simplified representation of the equilibrium of forces in a galaxy.

matter (which are hard to justify for a matter excepted by its qualificatif of "exotic"): it is not sensitive to electromagnetic force, it cannot absorb, reflect or emit light, it interacts with particles but very slightly. One also can add that this field allows explaining how DM extends to the whole Universe. Contrary to the first component of gravity, the gravitic fields $\boldsymbol{k}_0$ of galaxies' clusters can be combined on large distance just like the atomic spins are combined to generate a magnetic field at the scale of the whole material in EM. In GR case, the clusters' spins ($\boldsymbol{k}_0$) would play the role of the atomic spins and the Universe the role of the material.

Whatever one thinks about the validity of this hypothesis, one really thinks that it is very instructive first to accept without any justification this gravitic field k_0 that embeds the clusters and in particular with the previous expected values (which are the ones that explain dark matter) and make a first read of this current article. The application of this gravitic field to WLM works so well that it could be a justification. After that, the read of (Le Corre, 2015) [3] will allow justifying these assumptions.

3. WLM's Case Explained by DM, 2nd Component of Cluster's Gravitational Field of GR

3.1. About WLM

Here are the main data we need to know about WLM galaxy (coming from observation). Figure 2 presents the HI velocity map observed by MeerKAT radio telescope (Yang *et al.* 2022) [1]. The green arrow shows the direction of WLM's proper motion. The negative radial velocities of WLM mean that the galaxy approaches us, *i.e.* the vector direction is toward us. We adopt a heliocentric radial velocity of $\boldsymbol{v}_{rad} \sim -130\ \mathrm{km\cdot s^{-1}}$ for WLM (Leaman *et al.* 2009) [10]. The total space velocity is of about $v_{space} \sim 300\ \mathrm{km\cdot s^{-1}}$.

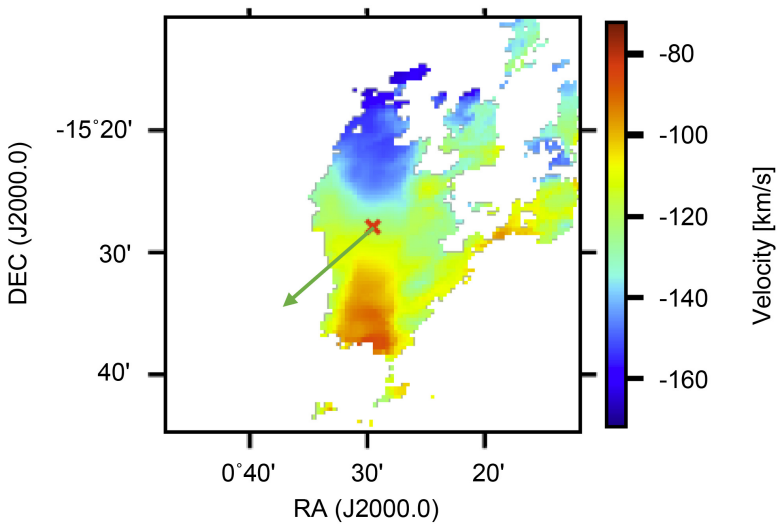

Figure 2. Meer KAT HI velocity map (Y. Yang *et al.* 2022) [1]. The green arrow shows the direction of WLM's proper motion. The red cross indicates the optical center of WLM.

We name the approaching side, the northern area of WLM (blue zone in Figure 2) which approaches faster than geometric center (red cross on Figure 2) and the receding side, the southern area of WLM (red zone in Figure 2) which approaches slower than geometric center.

The circular velocity (Figure 3) in the approaching side is about $v_{rot\_N} \sim 30\ \mathrm{km \cdot s^{-1}}$. The circular velocity in the receding side is about $v_{rot\_S} \sim 40\ \mathrm{km \cdot s^{-1}}$ (Khademi, 2021) [11].

We are going to explain the four trailing, extended gas clouds lying in the direction opposite to WLM's spatial motion in four steps of a geometric reasoning. Three parameters intervene in our explanation, proper motion $\boldsymbol{v}_{space}$, rotational velocity $\boldsymbol{v}_{rot}$ and gravitic field $\boldsymbol{k}_0$ in the Local Group. They combined themselves in four effects, 1) displacement due to proper motion for Ram pressure, 2) displacement due to proper motion with gravitic field, 3) displacement due to rotational velocity with gravitic field, 4) rotation due to rotational velocity. The first displacement and the last rotation are effects due to known physics, the two intermediary displacements are only expected by the DM solution.

Let's assume that the gravitic field $\boldsymbol{k}_0$ is oriented vertically. We will see hereafter that our solution is steady for a large interval of orientation of $\boldsymbol{k}_0$. This perpendicular orientation is then certainly not the real orientation and we will define an interval of possible orientation for $\boldsymbol{k}_0$ at the end of this study.

3.2. Step 1: Displacement Due to Proper Motion and Ram-Pressure

This step describes the Ram pressure. Because the gravitational force at the center of the galaxy is great compare to Ram pressure, one considers that environment pressure is only nonnegligible on a ring of matter at the end of WLM

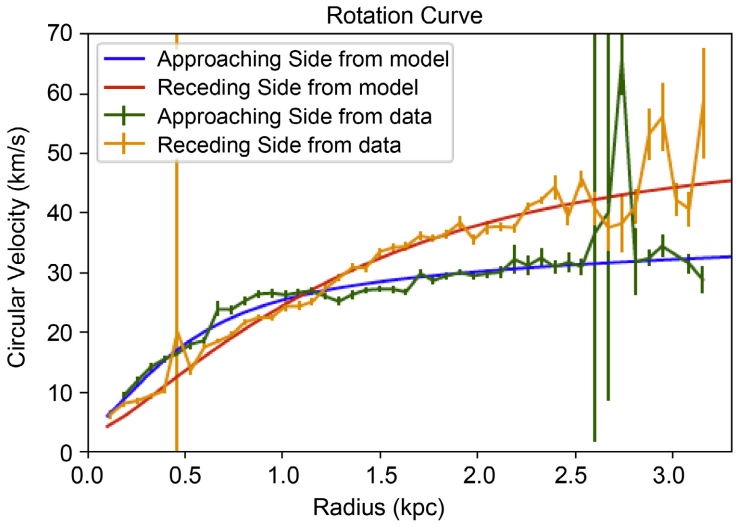

Figure 3. (Khademi, 2021) [11] Asymmetric rotation curve extracted from the perturbed halo potential (lopsided halo potential) model and from the observational data (Kepley *et al.* 2007) [2] for the approaching and the receding sides of WLM.

represented by the two ellipses in Figure 4. The external ellipse encloses the main body of the WLM HI (Y. Yang *et al.* 2022) [1]. The internal ellipse is defined graphically to be able to recover the main part of the four stripped clouds.

In Figure 4, we represented the move of the elliptical ring of the gas that undergoes Ram pressure which is slowing down by the environment pression along the proper motion of WLM. This movement due to proper motion is then constrained (for this first step) to stay on the red line (Figure 4) that figures the proper motion. One defines graphically this movement (black arrow in Figure 4) by starting at the geometric center of WLM and by ending at the horizontal of the higher vertical current position of the four stripped clouds (the two black dashed horizontal lines in Figure 4). This horizontal ending is not arbitrary but necessary because it is due to the verticality assumption of $\boldsymbol{k}_0$ which implies (next step) a horizontal force (or displacement).

First important result: By this way, it can be noticed that the observed stripped clouds are not strictly along the proper motion but slightly moved to the right of the proper motion axis. This observation is important because it means that the gas do not only undergo a Ram pressure but have a non-negligible motion component to the right. WLM would then be subjected to an unexpected force. This dark matter solution necessarily applies such a new force, which is the subject of the next steps.

3.3. Step 2: Displacement Due to Proper Motion and Gravitic Field k_0

Let's now apply the effect of the proper motion $\boldsymbol{v}_{space}$ with the gravitic field. Because of the mathematical expression of the force of the gravitic field, $\boldsymbol{F}_k = 4\boldsymbol{v}_{space} \wedge \boldsymbol{k}_0$, only a component perpendicular to the vertical $\boldsymbol{k}_0$ acts.

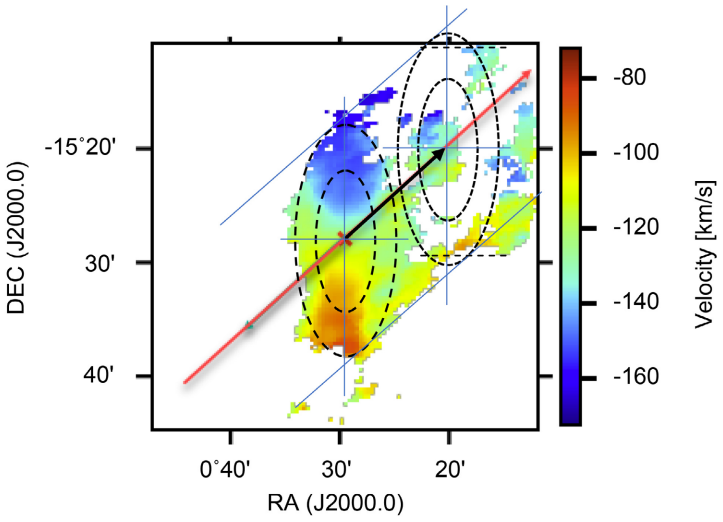

Figure 4. Displacement of the elliptical ring at the end of WLM that mainly undergoes Ram pressure. Ram pressure stripping acts along the proper motion axis (red arrow). Black arrow represents the displacement of HI gas ring.

Consequently, only a horizontal movement is allowed in 2D sky projection (that's why in the previous step we deduced the end of the movement on the black dashed horizontal lines). In a 2D representation as in Figure 5, only the effect of the radial velocity of the galaxy (in our line of sight) can be visible. Indeed, the component of proper motion in the perpendicular plane to the line of sight generates a force $\boldsymbol{F}_k$ parallel to the line of sight. It would only act by bringing gas closer or further along the line of sight but without deviating to the right or left. In this 2D representation (projection), one then cannot see any change from this component. Only the component of proper motion along the line of sight can generate a deviation to the right or left from our point of view (*i.e.* the heliocentric radial velocity $\boldsymbol{v}_{rad} \sim -130\ \mathrm{km \cdot s^{-1}}$). Because of the negativity of $\boldsymbol{v}_{rad}$ (WLM globally approaching us), one deduces that there is a component of proper motion in our line of sight which is in our direction (toward us). With our assumption of a vertical $\boldsymbol{k}_0$, one can then deduce from the mathematical expression $\boldsymbol{F}_k = 4\boldsymbol{v}_{rad} \wedge \boldsymbol{k}_0$, that the orientation of $\boldsymbol{k}_0$, in this case, is down. In Figure 5, we move the elliptical ring to be graphically adjusted on the four clouds thanks to this force's component:

Because this step uses gravitic field $\boldsymbol{k}_0$, this is the first effect of this "dark matter". The step 3 will be the second effect of "dark matter". But before the step 3, let's show that the observation of a shift on the right of the proper motion axis is already likely.

Clue about a Shift on the Right of the Proper Motion Axis for the Four Clouds

In (Y. Yang *et al.* 2022) [1], the authors propose a simulation of the Ram pressure in WLM (Figure 6).

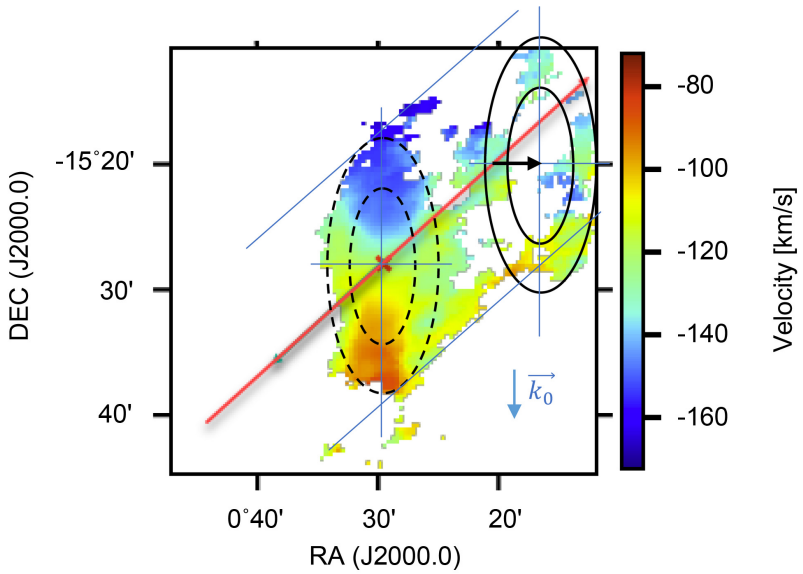

Figure 5. Displacement (black arrow) of the elliptical HI ring due (step 1) to environment pression along proper motion and (step 2) to proper motion and gravitic field $\boldsymbol{F}_{k,gal} = 4\boldsymbol{v}_{space} \wedge \boldsymbol{k}_0$.

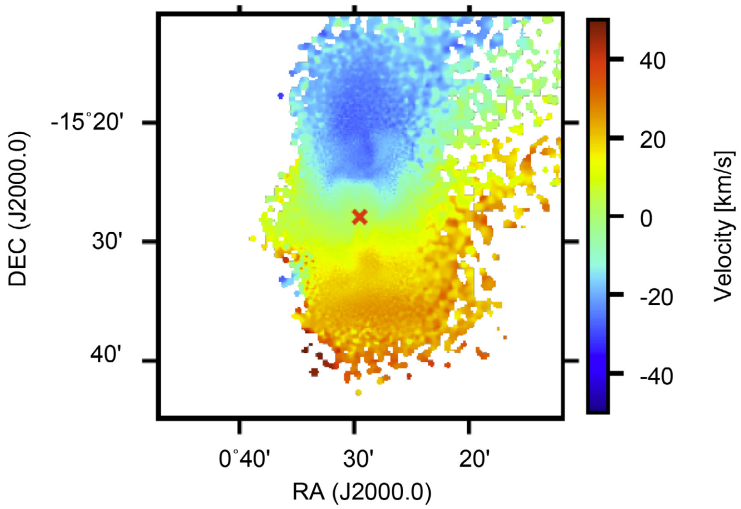

Figure 6. (Yang *et al.*, 2022) [1] Velocity map for a simulation of Ram pressure that uses a space velocity of 500 km·s^{-1} for WLM and an intergalactic medium density of 4×10^{-6} atoms cm^{-3}.

If one superimposes (**Figure 7**) their two figures, **Figure 6** and **Figure 2**, one can also remark that the eastern cloud but in particular the southern cloud are not completely recovered by the Ram pressure movement (left in **Figure 7**). But by applying a horizontal movement equivalent to the one of step 2 at the simulated HI gas striped by Ram pressure, the parallelogram, which localizes the gas due to Ram pressure, recovers very well the four clouds (right in **Figure 7**).

Remark: One only talks about "clue" because, at the current precision, if one takes in account the one-sigma error of the proper motion, on one side this shift could be greater but on the other side, it could be less and perhaps disappearing. But in our solution, the shift is expected, only except if $\boldsymbol{k}_0$ is perpendicular to the proper motion but we will see that it shouldn't be the case.

3.4. Step 3: Displacement Due to Rotational Velocity of WLM and Gravitic Field k_0

This step is equivalent to step 2 but now the gravitic force is obtained with the component of the rotational velocity $\boldsymbol{v}_{rot}$ of WLM galaxy, $\boldsymbol{F}_{k,rot} = 4\boldsymbol{v}_{rot} \wedge \boldsymbol{k}_0$. Graphically, one remarks that the position of the elliptical ring in the previous step contains the four stripped clouds (**Figure 5**). This step must then slightly move our elliptical ring. Let's compare the order of magnitude of the force applied in this step compare to the previous one. The force in the previous step was $\left\|\boldsymbol{F}_{k,gal}\right\| = 4\left\|\boldsymbol{v}_{space} \wedge \boldsymbol{k}_0\right\| \sim 4v_{rad}k_0$ because the angle between vertical $\boldsymbol{k}_0$ and $\boldsymbol{v}_{rad}$ (on our line of sight) is around 90˚. The force in current step due to the inner rotational velocity is $\left\|\boldsymbol{F}_{k,rot}\right\| = \left\|4\boldsymbol{v}_{rot} \wedge \boldsymbol{k}_0\right\| \sim 4v_{rot}k_0 \sin\left(\widehat{\boldsymbol{v}_{rot}, \boldsymbol{k}_0}\right)$. The angle between vertical $\boldsymbol{k}_0$ and $\boldsymbol{v}_{rot}$ at the extremity north and south of the ellipse is around 90˚, as one can see that in **Figure 8**. It gives $\left\|\boldsymbol{F}_{k,rot}\right\| \sim 4v_{rot}k_0$. One deduces that $\frac{\left\|\boldsymbol{F}_{k,rot}\right\|}{\left\|\boldsymbol{F}_{k,gal}\right\|} \sim \frac{v_{rot}}{v_{rad}}$ at the extremity north and south. At the northern

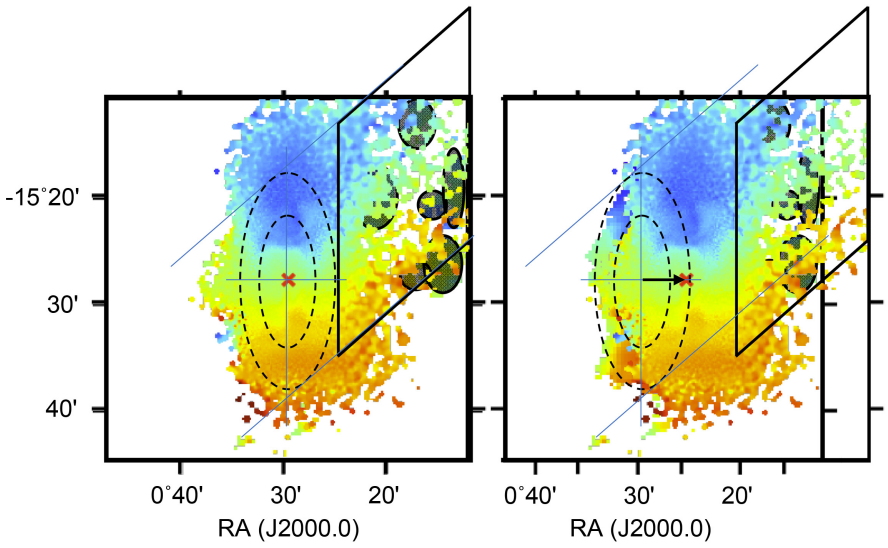

Figure 7. *On left*: Superposition of simulation of Ram pressure (**Figure 6**) on real distribution of HI gas (**Figure 2**). The parallelogram indicates the area HI gas striped by Ram pressure. The filled in black ellipses recover the four clouds. *On right*: Idem with a translation of the parallelogram equivalent to step 2.

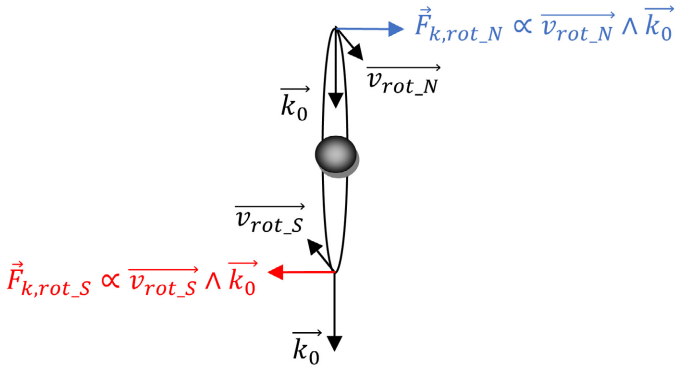

Figure 8. Simplified representation of the gravitic forces in a **highly inclined galaxy** as in WLM.

approaching side $\frac{\|\boldsymbol{F}_{k,rot\_N}\|}{\|\boldsymbol{F}_{k,gal}\|} \sim \frac{v_{rot\_N}}{v_{rad}} \sim \frac{30}{130} = 1/4.35$ and at the southern receding side $\frac{\|\boldsymbol{F}_{k,rot\_S}\|}{\|\boldsymbol{F}_{k,gal}\|} \sim \frac{v_{rot\_S}}{v_{rad}} \sim \frac{40}{130} = 1/3.25$.

If one looks at the two extremities of the roughly horizontal minor axis of the elliptical ring (red point in **Figure 8**), the rotational speeds ($\boldsymbol{v}_{rot\_E}$ at east and $\boldsymbol{v}_{rot\_W}$ at west) are vertical like $\boldsymbol{k}_0$ (and also null in our line of sight). This quasi collinearity means that $\|\boldsymbol{F}_{k,rot\_EW}\| = \|4\boldsymbol{v}_{rot\_E} \wedge \boldsymbol{k}_0\| \sim \|4\boldsymbol{v}_{rot\_W} \wedge \boldsymbol{k}_0\| \sim 0$. From these ratios and because we know graphically the effects of $\|\boldsymbol{F}_{k,gal}\|$ (black arrow of step 2) one can report the effects of $\|\boldsymbol{F}_{k,rot}\|$ on the northern approaching side (adding a movement to the right) and southern receding side (adding a movement to the left). The force is applied horizontally. On **Figure 9**, these

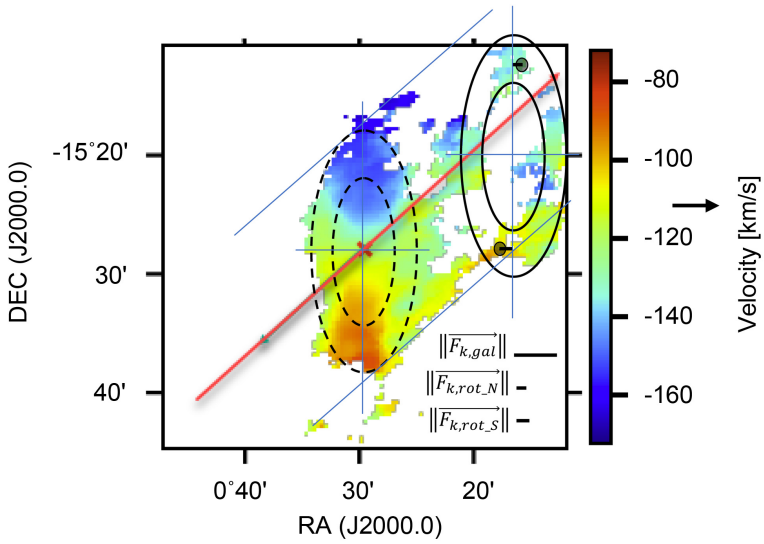

Figure 9. Displacements of the northern and southern clouds of the elliptic ring represented at the scale of the graphic ($\boldsymbol{F}_{k,rot} = 4\boldsymbol{v}_{rot} \wedge \boldsymbol{k}_0$). Final positions are materialized by the 2 black points.

movements are represented at the scale of the graphic and the final positions of the northern and southern clouds in the elliptic ring are materialized with the 2 black points. These points (due to these forces) should be roughly at the center of gravity of the two clouds (north and south). But one has to observe that they don't really match.

3.5. Step 4: Rotation Due to Rotational Velocity of WLM

By a pragmatic attitude (but probably because it is physically required as we will see hereafter), a way to enhance the situation would be to turn globally the ring as it is done in **Figure 10** for which a turn counterclockwise of about 10˚ is applied:

We don't know the value of the rotation (which does not depend from $\boldsymbol{k}_0$) but graphically it should be between around 10˚ and 20˚.

This "a priori pragmatic" counterclockwise rotation is interesting in several ways. Firstly, this global turn is not only conceivable but certainly required by the physics because the gas pulled out of the galaxy continues to spin. Inside the galaxy, the ring is seen as a "continuous fluid" (without hole) and we don't distinguish the rotation of the homogeneous fluid (in its globality). But in the ring of stripped gas, the clouds are individualized (we will see how hereafter) which allows to follow them in the rotation.

Secondly, in addition to allowing to get a better fit of black points (**Figure 10**) on the centers of the clouds, it also seems to give a roughly better alignment of the ring with the iso velocities (**Figure 11**) of the clouds. In **Figure 11**, one has drawn in yellow several iso velocities of the four clouds that tend to stay straight. Firstly, it really seems to show a rotation compare to the ones in the galaxy. Second, this rotation appears to be counterclockwise as expected by our graphical determination. But this consequence must be confirmed by more accurate observations.

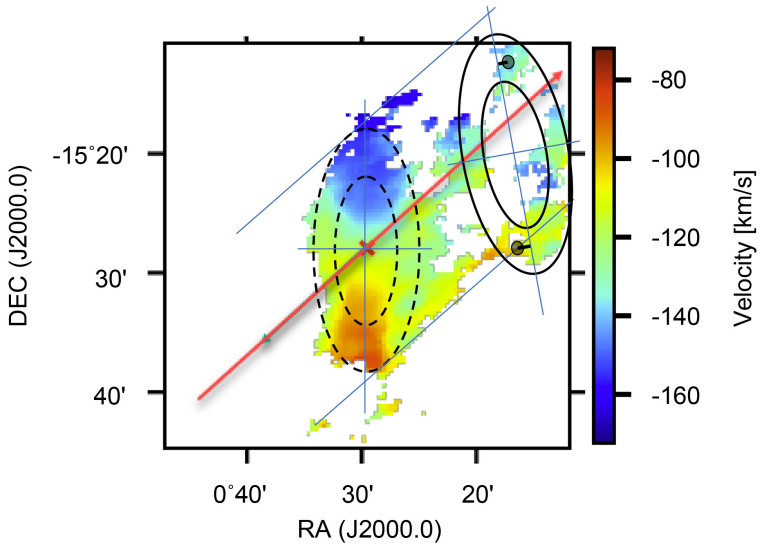

Figure 10. The HI gas pulled out of the galaxy continues to spin generating a rotation of the fluid in its globality. This effect is independent of the gravitic field $\boldsymbol{k}_0$.

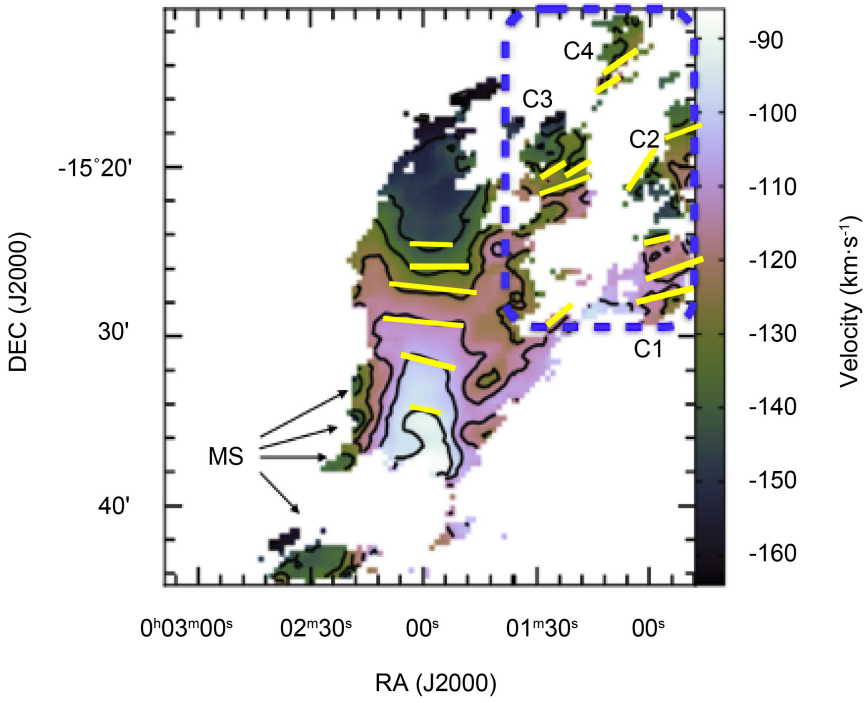

Figure 11. (Yang et al., 2022) Velocity field of WLM from the MeerKAT observations. The four discovered clouds, *i.e.*, C1, C2, C3, and C4, and the contamination from the Magellanic Stream (MS) are indicated. The blue dashed-line box encloses the four clouds. Yellow lines indicate several iso velocities of the four clouds that tend to stay straight and showing a rotation compared to iso velocities in WLM galaxy.

Our solution leads then to a prediction:

Second important result: The four clouds of WLM (and their iso velocities) should undergo a counterclockwise rotation around the center of the elliptic ring.

Furthermore, there is another consequence of this counterclockwise rotation. To be able to rotate counterclockwise (on 2D projection on the sky) with a northern approaching side and a southern receding side, it implies that the left side of WLM is toward us and the right side is in the background.

Third important result: the left side of WLM is toward us and the right side is in the background.

One can insist that this rotation is not a consequence of the gravitic field. It should then exist even if this explanation of dark matter would be wrong (even if $\boldsymbol{k}_0$ isn't large enough).

3.6. From a Homogeneous Elliptical Ring to the Four Individualized Clouds

These previous considerations lead us to seek to understand how these clouds were individualized. Until now, one moved the elliptical ring in its globality. It means that the gas at this step would be uniformly distributed inside the ring. But we have just seen that the approaching and receding sides undergo two not null forces (and even two opposite forces because of the sign of the radial velocity, Figure 12) and also that the forces at east and west on the minor axis of elliptical ring are null ($\left\|\boldsymbol{F}_{k,rot\_EW}\right\| \sim 0$). While the balance of power between $\left\|\boldsymbol{F}_{k,rot\_S}\right\|$ or $\left\|\boldsymbol{F}_{k,rot\_N}\right\|$ and $\left\|\boldsymbol{F}_{k,gal}\right\|$ makes $\left\|\boldsymbol{F}_{k,rot\_S}\right\|$ and $\left\|\boldsymbol{F}_{k,rot\_N}\right\|$ very weak for the global movement, the ratio between $\left\|\boldsymbol{F}_{k,rot\_S}\right\|$ or $\left\|\boldsymbol{F}_{k,rot\_N}\right\|$ and $\left\|\boldsymbol{F}_{k,rot\_EW}\right\|$ is great for the local movement. It makes $\left\|\boldsymbol{F}_{k,rot\_EW}\right\|$ negligible for the inner distribution of the gas compare to $\left\|\boldsymbol{F}_{k,rot\_S}\right\|$ or $\left\|\boldsymbol{F}_{k,rot\_N}\right\|$. Concretely, the approaching and receding sides undergo a force that slightly stretch the gas at the north and south areas (around the black points), while the east and west areas don't undergo

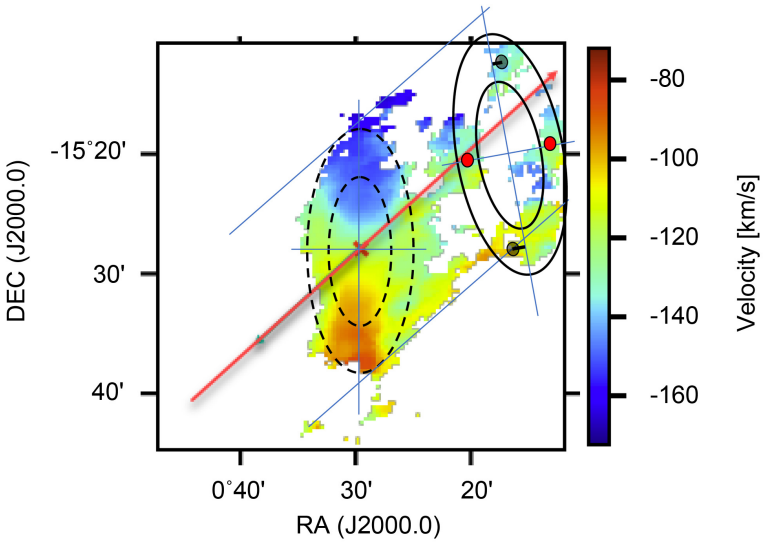

Figure 12. Four different dynamics located at the four cardinal points of the elliptical ring generating four separated clouds: the two black points have opposite gravitic forces, $\boldsymbol{F}_{k,rot\_S} \sim -\boldsymbol{F}_{k,rot\_N}$ and the two red points have null gravitic forces $\boldsymbol{F}_{k,rot\_EW} \sim \boldsymbol{0}$.

such a force (around the red points). Gradually, these two vertical sides deviate from the horizontal eastern and western sides generating four separated clouds of gas at the four extremities of the elliptical ring. Inside the ring of gas, there are four different dynamics located at the four cardinal points of the ellipse and between them the gas tears.

Fourth important result: This DM solution can explain the four clouds of WLM at the four cardinal points of the ellipse.

3.7. Two of the Four Stripped Clouds Show a Bridge with WLM

The observations show two bridges between the galaxy and two of the four clouds. These bridges and their number can also be explained by these movements in 3D space. Because of the direction toward us of the proper motion, the four clouds of the four extremities of the elliptical ring are not only moving up and right but are also pushing back by the environment's pression. This movement in the depth of the 3D space makes the south closer to the center of WLM than the north, letting southern cloud undergoes the gravitational influence of WLM. And, depending on whether the right side is in front or behind the left side (in 3D space), one or the other of the two clouds on the minor axis should also be closer than the other to the center of WLM. This gravitational proximity to WLM of these two areas can explain the two bridges. One can precise that from our third result, the bridge should be on the cloud toward us.

One can notice the consistency of the solution. If the proper motion v_{rad} had been positive (with the same others velocities), the southern cloud would perhaps not have a bridge because it would move away from the center of WLM like the northern cloud. There would only be one bridge. And by the same time the movement of the elliptical ring (resulting from step 2) would not lead to locate the ring under the proper motion axis (by a movement on the right) but above the proper motion axis (by a movement on the left) which is not what we observe, but two bridges and a shift to the right of the four clouds.

Fifth important result: This DM solution can explain the two bridges between WLM and two of the four HI clouds.

3.8. Quantitative Deductions of the Densities of WLM and Its Environment and of Dark Matter

Until now, we have mainly geometrically explained the four stripped clouds. We are now going to obtain quantitative results to consolidate and ensure the consistency of this explanation of dark matter on WLM.

The previous step 1 is due to the Ram pressure of the environment on WLM. The step 2 is due to the gravitic force obtained by the proper motion of WLM. Let's note ρ_{IGM} the density of matter of the environment (the Inter Galactic Medium) and ρ_{ISM} the density of matter of the WLM galaxy in the elliptical ring (around the last kiloparsec at the end of the galaxy, its size is then around $R_{ring} \sim 1\,\text{kpc}$). If we consider that the energy E_{IGM} given to the particles of IGM

(for Ram pressure) is of the order of magnitude of the energy E_{ISM} produce by the gravitic force in the ring, (in this solution it is justified because the displacement in step 1 and in step 2 are of the same order of magnitude) one can write:

$$E_{IGM} \sim E_{ISM} \Rightarrow \rho_{IGM} v_{space}^2 = \rho_{ISM}\, 4k_0 v_{rad} R_{ring} \Rightarrow \frac{\rho_{IGM}}{\rho_{ISM}} = 4k_0 \frac{v_{rad}}{v_{space}^2} R_{ring}$$

In (Le Corre, 2015) [3], to be able to explain the dark matter of the galaxies on the 16 studied samples, the deduced value of the gravitic field k_0 of a cluster is in the following interval, $10^{-16.62} < k_0 < 10^{-16.3}$. Because WLM is at the edge of the cluster, k_0 should be around the minimum of this interval. Let's take $k_0 \sim 10^{-16.62}\ \mathrm{s}^{-1}$. With $R_{ring} \sim 1\ \mathrm{kpc} \sim 3\times10^{19}\ \mathrm{m}$, $v_{rad} \sim 130\ \mathrm{km\cdot s^{-1}} \sim 1.3\times10^5\ \mathrm{m\cdot s^{-1}}$, $v_{space} \sim 300\ \mathrm{km\cdot s^{-1}} \sim 3\times10^5\ \mathrm{m\cdot s^{-1}}$, one obtains:

$$\frac{\rho_{IGM}}{\rho_{ISM}} = 4\times10^{-16.62} \times \frac{1.3\times10^5}{9\times10^{10}} \times 3\times10^{19} \sim 10^{-2.62} \sim 10^{-3}$$

Since we work in order of magnitude and despite the gravitic field $\boldsymbol{k}_0$ is not precisely known, our solution allow to obtain a not so bad value of the ratio of the density of HI atoms $\frac{n_{IGM}}{n_{ISM}}$ with the IGM volume density n_{IGM} and the WLM volume density at the end of the galaxy n_{ISM}. Indeed, if $n_{IGM} \sim 10^{-4}\ \mathrm{atoms\cdot cm^{-3}}$, it gives $n_{ISM} \sim 10^{-1}\ \mathrm{atom\cdot cm^{-3}}$ at the periphery of WLM. Furthermore, the value of $\|\boldsymbol{k}_0\|$ from (Le Corre, 2015) [3] is obtained from only 16 galaxies. Consequently, the interval of k_0 is likely a minimal interval. The lower limit of k_0 is then probably less than $k_0 \sim 10^{-16.62}\ \mathrm{s}^{-1}$ which will decrease the ratio $\frac{n_{IGM}}{n_{ISM}}$.

Sixth important result: This DM solution can obtain the ratio of the density of HI atoms $\frac{n_{IGM}}{n_{ISM}} < 10^{-3}$ at the end of the galaxy.

This result is very important because it allows to retrieve volume density with a parameter k_0 used in two different contexts: one to explain the dark matter, *i.e.* the rotation speeds at the ends of galaxies (with the previous expected value) and the other to explain the ram pressure observed on WLM case with its four stripped clouds of HI gas away from WLM. Furthermore, with this solution there is no dark matter halo. The galaxy's mass is then only composing of the baryonic particle. In (Yanbin Yang *et al.*, 2022) [1], the authors find that their numerical models only provide good matches to the observations (for Ram pressure effect) when they adopt very low total masses for WLM. This solution, by eliminating the dark matter, eliminates the hypothetical but the main component of its dynamical mass.

Seventh important result: The value of k_0 calculated in (Le Corre, 2015) [3] to obtain the rotational speeds at the end of the galaxies is relevant because allowing retrieving the ratio of the density of HI atoms $\frac{n_{IGM}}{n_{ISM}}$

Remark: Inversely to our computation, when a physical situation combines the effects of Ram pressure and gravitic field, the measure of the ratio of densities could be a way to measure the gravitic field.

The capacity of this explanation of dark matter to explain the case of WLM seems to confirm that the gravitic field would certainly be generated by the galaxies' clusters. Indeed, to retrieve the good order of magnitude of the volume densities in the case of WLM, the gravitic field must be weak enough. The minimal value of gravitic field (if it is generated by the galaxies' clusters) must then locate at the end of the clusters. WLM is precisely located at the edge of a cluster.

Eighth important result: The origin of $\boldsymbol{k}_0$ as the gravitic field of the cluster is corroborate by WLM's case.

Remark: If this dark matter solution is confirmed, then one way to determine the boundaries of a cluster could be the geometrical locations of the physical minimum of gravitic field $\|\boldsymbol{k}_0\|$.

3.9. About the Orientation of k_0 the Gravitic Field of the Cluster

As written at the beginning of this study, we are going to show that the assumption of the verticality of $\boldsymbol{k}_0$ is not too constraining. It exists in fact a large interval of possible $\boldsymbol{k}_0$. The orientation of $\boldsymbol{k}_0$ concerns directly the step 2 and 3 but also indirectly the step 1 by the intermediary of the step 2. Indeed, by rotating the gravitic field $\boldsymbol{k}_0$, the movement $\boldsymbol{F}_{k,gal} = 4\boldsymbol{v}_{space} \wedge \boldsymbol{k}_0$ of step 2 (Figure 13) also rotates around the final expected position of step 2. The final expected position, black cross in Figure 13, is always the same whatever the angle of $\boldsymbol{k}_0$ in particular

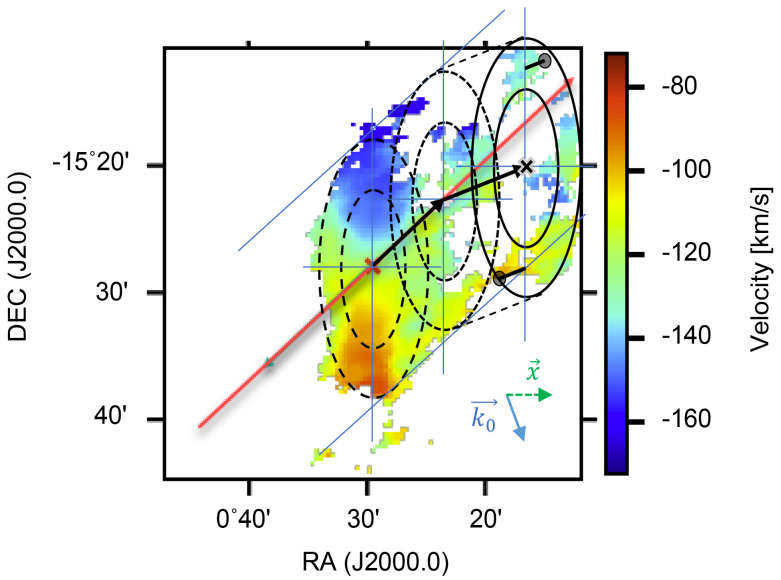

Figure 13. Example of an orientation of $\boldsymbol{k}_0$ with $\left(\widehat{\boldsymbol{x},\boldsymbol{k}_0}\right) = -70^\circ$ (different from our previous studied case $\left(\widehat{\boldsymbol{x},\boldsymbol{k}_0}\right) = -90^\circ$). For visibility, only the 3 displacements of the 3 first steps are represented.

because at the step 3 the minor horizontal axis has a null force (as seen before $\boldsymbol{F}_{k,rot\_EW} \sim \boldsymbol{0}$). It then modifies the length of the movement of step 1. On Figure 13, one applies this rotation of $\boldsymbol{k}_0$ to the movement $\boldsymbol{F}_{k,rot} = 4\boldsymbol{v}_{rot} \wedge \boldsymbol{k}_0$ of step 3. The values of the angles of $\boldsymbol{k}_0$ are given compare to the horizontal axis oriented to the right (noted $\boldsymbol{x}$ below) with a positive sign for counterclockwise. One also applies the scales calculated at step 3 to the length of the forces at the center of mass at north and south ($\frac{\left\|\boldsymbol{F}_{k,rot\_N}\right\|}{\left\|\boldsymbol{F}_{k,gal}\right\|} \sim \frac{v_{rot\_N}}{v_{rad}} \sim \frac{30}{130} = 1/4.35$ and $\frac{\left\|\boldsymbol{F}_{k,rot\_S}\right\|}{\left\|\boldsymbol{F}_{k,gal}\right\|} \sim \frac{v_{rot\_S}}{v_{rad}} \sim \frac{40}{130} = 1/3.25$). For the visibility of the figures, one hasn't applied the last rotation of the whole gas ring (step 4). It is also because it doesn't depend of $\boldsymbol{k}_0$ and furthermore we don't know the value of this rotation.

A priori, the interval of possible $\boldsymbol{k}_0$ contains all possible directions, that is $-360^\circ < \left(\widehat{\boldsymbol{x},\boldsymbol{k}_0}\right) < 0^\circ$. On Figure 14, several characteristic orientations are represented, allowing to reduce the possible orientations of $\boldsymbol{k}_0$. From the Ram pressure intensity, the first extreme case, for which there is no Ram pressure, defines the first limit of the interval of $\left(\widehat{\boldsymbol{x},\boldsymbol{k}_0}\right) \sim -55^\circ$; the second extreme case (asymptotic limit) for which $\boldsymbol{F}_{k,rot\_S}$ and $\boldsymbol{F}_{k,rot\_N}$ are parallel to Ram pressure (infinite vectors), defines the second limit of the interval of $\left(\widehat{\boldsymbol{x},\boldsymbol{k}_0}\right) \sim -225^\circ$; This first reduction of the interval of possible $\boldsymbol{k}_0$ (from Ram pressure possible intensity) leads to the possible interval $-225^\circ < \left(\widehat{\boldsymbol{x},\boldsymbol{k}_0}\right) < -55^\circ$.

Others remarkable configurations are represented: with $\boldsymbol{F}_{k,rot\_S}$ and $\boldsymbol{F}_{k,rot\_N}$ perpendicular to proper motion axis ($\left(\widehat{\boldsymbol{x},\boldsymbol{k}_0}\right) \sim -135^\circ$); with $\boldsymbol{F}_{k,rot\_S}$ and $\boldsymbol{F}_{k,rot\_N}$ vertically ($\left(\widehat{\boldsymbol{x},\boldsymbol{k}_0}\right) \sim -180^\circ$); and two intermediary configurations ($\left(\widehat{\boldsymbol{x},\boldsymbol{k}_0}\right) \sim -70^\circ$ and $\left(\widehat{\boldsymbol{x},\boldsymbol{k}_0}\right) \sim -200^\circ$).

The second extreme case is where $\boldsymbol{k}_0 \sim -225^\circ$. At this limit, the movement of step 2 is nearly parallel to proper motion, it is then impossible at the step 2 to retrieve the final expected position (except with infinite displacements). And beyond this angle, step 2 generates a movement upper the proper motion axis contrary to the final expected position (under the proper motion axis).

The application of the scale of step 3 is important because it also allows reducing the previous interval because at its limits (for $\left(\widehat{\boldsymbol{x},\boldsymbol{k}_0}\right) \sim -225^\circ$ and $\left(\widehat{\boldsymbol{x},\boldsymbol{k}_0}\right) \sim -55^\circ$) the positions of the centers of mass of the northern and southern clouds are completely false, *i.e.* this solution is irrelevant around these limits. This second reduction of the interval of $\boldsymbol{k}_0$ (from this DM solution applied on rotational speeds of WLM) leads roughly to the more reasonable possible interval $-200^\circ < \left(\widehat{\boldsymbol{x},\boldsymbol{k}_0}\right) < -70^\circ$.

At this step, this DM solution on WLM is then possible for the following interval of orientation of $\boldsymbol{k}_0$:

$$-200^\circ < \left(\widehat{\boldsymbol{x},\boldsymbol{k}_0}\right) < -70^\circ \Leftrightarrow 160^\circ < \left(\widehat{\boldsymbol{x},\boldsymbol{k}_0}\right) < 290^\circ$$

Once again, the rotation of step 4 (independent from $\boldsymbol{k}_0$) hasn't been applied.

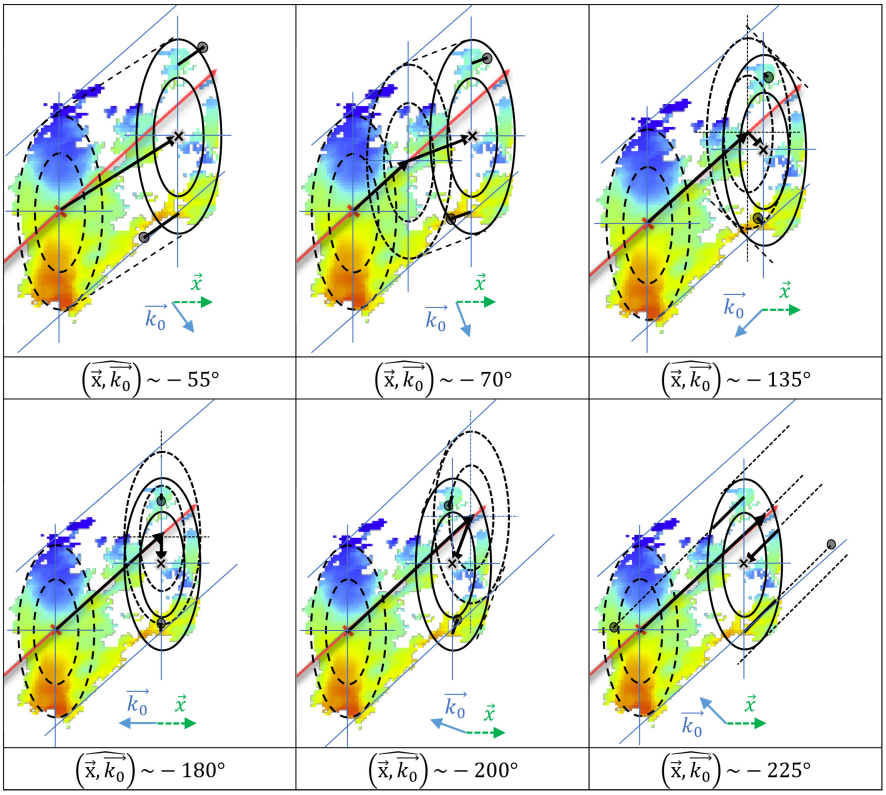

Figure 14. Forces exerted in WLM's case for several possible orientations of the gravitic field $\boldsymbol{k}_0$.

But one can note that the application of this rotation enhances, for a shorter interval, the position of the points in the figures compare to the center of mass of the four clouds. We will see now from another characteristic of this DM solution that one can effectively reduce the interval around $\left(\widehat{\boldsymbol{x},\boldsymbol{k}_0}\right) \sim -180^\circ$.

Dwarf Satellites Alignments and Gravitic Field k_0

One can still refine our result on the interval of $\boldsymbol{k}_0$ because this explanation of dark matter implies (Le Corre, 2015) [3] the alignment in a plane of the dwarf satellites around their host galaxy. Furthermore, this plane is expected to be perpendicular to the gravitic field $\boldsymbol{k}_0$ of their cluster of galaxies. In Our Local Group, several such alignments have been observed. Around M31 (Ibata *et al.* 2013) [12] and around Milky Way (Pawlowski *et al.* 2012) [13]. In the two cases, the plane of alignment is near to the perpendicular to Milky Way (MW) with angles less than 20˚. In our figures of WLM, $\boldsymbol{x}$ is roughly the galactic plane of MW. One can then expect that the gravitic field $\boldsymbol{k}_0$ of our Local Group is roughly at an angle less than 20˚ around MW galactic plane. This DM solution implies:

Ninth important result: The gravitic field $\boldsymbol{k}_0$ (which represents the dark matter) of our Local Group would be roughly in the interval $160^\circ < \left(\widehat{\boldsymbol{x},\boldsymbol{k}_0}\right) < 200^\circ$ (*i.e.* oriented roughly along MW galactic plane in an interval of around ±20˚).

It is remarkable that this narrow interval is consistent with our previous de-

duced interval. In this narrow interval of $\boldsymbol{k}_0$, the counterclockwise rotational effect of step 4 (not represented in Figure 14) enhances the position of the ellipse compare to the four clouds.

One can remind that the alignment of the orbital trajectories of dwarf satellites is unexpected with traditional DM assumption (as an exotic matter) while in this DM solution, it is expected.

Remark: A more recent publication (Müller *et al.* 2018) [14] find also evidence for a kinematically coherent plane of satellite galaxies around Centaurus A.

Let's note once again the consistency of this solution. Because WLM is expected to be isolated and because it is a dwarf galaxy (*i.e.* light galaxy), its own equatorial plane is susceptible to be mainly influenced by $\boldsymbol{k}_0$ (*i.e.* such that $\boldsymbol{v}_{rot}$ is perpendicular to $\boldsymbol{k}_0$ because $\boldsymbol{F}_{k,rot} = 4\boldsymbol{v}_{rot} \wedge \boldsymbol{k}_0$). The fact that WLM galactic plane is close to the perpendicular to the MW (*i.e.* to $\boldsymbol{k}_0$) is then consistent with this DM solution.

Tenth important result: The orientation of WLM galactic plane perpendicular to $\boldsymbol{k}_0$ (*i.e.* to the MW) can be explained by this solution of DM because of its isolated position and evolution (far from influence of other galaxies and mainly undergoing the effect of $\boldsymbol{k}_0$).

3.10. Another Deduction: The Warping of WLM

Until now we focused on the four stripped clouds (external to WLM), let's see what happens in the galaxy itself. This gravitic field $\boldsymbol{k}_0$ (explaining dark matter) can also explain the warping of WLM. Let's first explain the warping in an advantageous situation such as Figure 15. As the gravitic force is $\boldsymbol{F}_k = 4\boldsymbol{v} \wedge \boldsymbol{k}_0$, with a uniform $\boldsymbol{k}_0$ along the galaxy, the force evolves then depending of the evolution of $\boldsymbol{v}$, *i.e.* of the gradient of $\boldsymbol{v}$. If the gradient is linear, the force will evolve linearly along the galaxy. The effects (depending of the angle of $\boldsymbol{k}_0$) will be a regular inclination without warping. But if the gradient is not regular, there are both inclination and warping (left on Figure 15).

In the particular case of WLM with its asymmetric velocity field, the approaching side appears to be warped and shows a steeper velocity gradient than the receding side in the inner region of the galaxy (Kepley, 2007) [2] as one can see that on Figure 16. It is the correlation that this DM solution expect, between

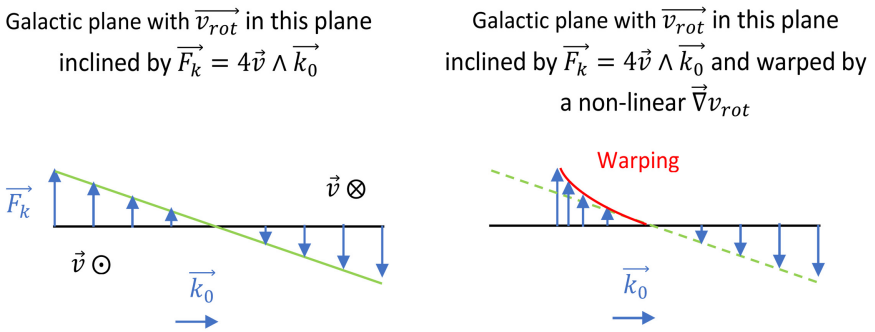

Figure 15. Warping and inclination of a galaxy from a gradient of rotational speed.

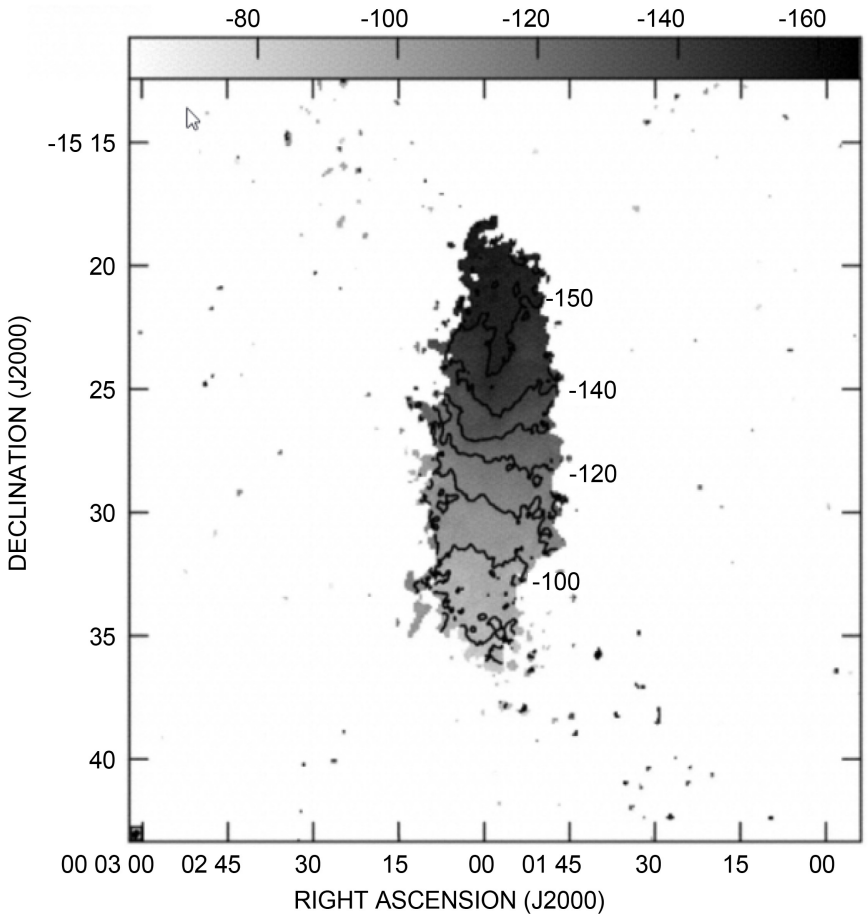

Figure 16. (Kepley, 2007) Mean-velocity map of WLM. The contour levels are −150, −140, −130, −120, −110, −100 and −90 km·s^{-1}.

geometrical warp and gradient of rotational velocities. In the case of WLM, because $\boldsymbol{k}_0$ is close to be perpendicular to WLM, this warping must be slight.

Eleventh important result: This solution of dark matter can explain that the steeper gradient of rotational velocity in northern side of WLM (compare to southern side) generates a warping of this northern side.

4. Discussion

4.1. About the Warping of MW and Its Precession

A phenomenon of precession has been suggested in the study of dark matter around the gravitic field $\boldsymbol{k}_0$ (Le Corre, 2015) [3], just like in EM with the magnetic field. Three recent publications (Poggio *et al.*, 2020) [15], (Cheng *et al.*, 2020) [16] and (Chrobáková, López-Corredoira, 2021) [17] observed that our galaxy's warp was spinning with a procession that would be faster than models had predicted. The fact that this precession is faster than expected could be explained by this DM component $\boldsymbol{k}_0$ because the gravitic field of the clusters would be in general underestimated (and perhaps also the own gravitic field of the galaxies). Indeed, in this solution it's not the matter that is missing but the 2nd

component of RG that is underestimated.

4.2. About Gravitic Field k_0

It is important to keep in mind that this gravitic field $\boldsymbol{k}_0$ is a characteristic which comes from GR (unknown in Newtonian gravitation) in the same way as the curvature of space and the gravitational waves. One can noticed that curvature of space is became very important elements of our knowledge and understanding of the universe. And the gravitational waves is an incredible window on a new reality as a sixth sense. It is very surprising that this gravitic field (this 3rd new characteristic of the universe revealed by GR also known as Lens-Thirring effect) is not highly valued until now. In this solution, this gravitic field would be the dark matter. It will then take an honorable place as well as curvature of space and gravitational waves. If we compare with EM, gravitic field corresponds to magnetic field. Once again, it will be very surprising that gravitic field cannot have the same importance that magnetic field in EM. One can also add that because $\boldsymbol{k}_0$ is unknown in Newtonian gravitation, GRL can be seen as a kind of MOND theory (but natively in agreement with GR).

4.3. About Exotic Matter Versus Gravitic Field k_0

4.3.1. Hypothesis 1: Nature of Dark Matter

To explain the gravitational issue detected from galaxies' scale and beyond, one assumes the existence of a matter never discovered to date. In this explanation of DM we don't create a new physical entity and don't modify current gravitational theory, we only use the gravitic field that exists for any object, it is then not a hypothesis at all because predicted by RG and already observed.

4.3.2. Hypothesis 2: Quantity of Dark Matter

The quantity of this exotic matter must represent at least 5 times the known matter. In other words, we have built theories to explain the behavior of known matter with very great precision and these theories would lead us to conclude that they are only able to explain 25% of reality (while this exotic matter surrounds us). If it was the case, we would rather be entitled to question the predictive capacity of such theories. In general, the unknown mass hypothesis is made when there is a small gap with respect to the theory (with matter which is always known matter) and this is what makes it possible to discover new objects (Neptune, exoplanets, etc.). For the gravitic field (which, let us remember, exists for any object), the only hypothesis in this attempt to explain dark matter is to assume that this field is larger than what was thought for certain objects. Moreover, to support this possibility of a larger than expected field, the example of the EM validates this solution. Indeed, this gravitic field is mathematically similar to the magnetic field. The EM experiment shows us that although objects can be neutral there are magnetic fields much higher than expected such as the magnetic fields of planets. But even more, the fact that it is not a central force, these fields can mutualize

each other to create large-scale magnetic fields (ferromagnetic material, magnet for example which sees their spin at the atomic level being maintained at the material scale). Such a field is then able to fill an environment (as in accelerators). These physical characteristics, which have no reason not to apply to the gravitic field, make it possible to explain dark matter. And now if we look at the value of the gravitic field necessary to find the amount of "dark matter", it turns out that it is still very low. So weak that locally no device is currently sensitive enough to measure it, explaining why this theory works well at local scale (this field being negligible). On the other hand, due to the mathematical nature of the force, $\boldsymbol{F}_k = 4\boldsymbol{v} \wedge \boldsymbol{k}_0$, high speeds or large distances (Le Corre, 2015) [3] are needed to detect its effect and these are precisely the physical scale where dark matter appears.

4.3.3. Hypothesis 3: Behavior of Dark Matter

DM is not sensitive to EM force, it cannot absorb, reflect or emit light. It interacts with particles very slightly (because we never detected it), but generates an excess of gravitation (because of its effects on large structures of our Universe). It is an invisible matter. All these characteristics are illogical for a matter (justifying the term of exotic matter), but they are all verified if DM is the gravitic field (2nd component of RG similar to magnetic field in EM).

One can add that dark energy could also be another facet of the gravitic field (Le Corre, 2015a) [18]. This is more hypothetical but some expected behaviors or observations can be explained as primordial inflation (Le Corre, 2020) [19] or anisotropies of CMB sky (Le Corre, 2021) [20].

5. Conclusions

In this paper, one studied WLM's case with a new dark matter explanation (Le Corre, 2015) [3] for which it is not an exotic matter but the 2nd component of the gravitation field of GR (giving the observed Lense-Thirring effect) named in this paper the gravitic field $\boldsymbol{k}_0$. This explanation doesn't need any more matter than the known baryonic matter. One uses several expected consequences of this DM solution already observed (and for some of them unexplained in the assumption of DM as an exotic matter): the existence of privileged alignments in a cluster, the warping of galaxies due to $\boldsymbol{k}_0$ and the orientation and value of $\boldsymbol{k}_0$ (*i.e.* the expected quantity of DM). With these key parameters of this DM solution, one explains:

- the four trailing, extended gas clouds, and their position around the four cardinal points of an ellipse (a DM effect)
- the position lying in the direction opposite to WLM's spatial motion (due to Ram pressure)
- the two bridges between WLM and two of the four clouds
- its approaching side appears to be warped (a DM effect)
- a steeper velocity gradient for the approaching side than for the receding side

in the inner region of the galaxy.

One also deduces (not expected or deducible by Ram pressure effect):

- a slight shift of the four clouds below the line of WLM's proper motion (a DM effect)
- a slight counterclockwise rotation of these clouds (should be revealed by the iso velocities of these four clouds)
- the left (western) side of WLM is positioned frontward and the right (eastern) side backward (deduced thanks to DM)
- the roughly vertical position of WLM roughly perpendicular to $\boldsymbol{k}_0$ (a DM effect)
- the orientation of the vector $\boldsymbol{k}_0$ (explaining DM) close to the galactic plane of Milky Way in an interval of around ±20˚
- the densities of interstellar gaseous medium (ISM) and gaseous intergalactic medium (IGM) (deduced thanks to DM).

WLM explanation and DM explanation together also confirm:

- the right quantity of DM (the good order of magnitude of the vector explaining DM $\boldsymbol{k}_0$)
- the origin of the vector $\boldsymbol{k}_0$, coming from galaxies' clusters.

Because this explanation of WLM's case and this explanation of DM are independent of each other, they demonstrate great relevancy of this DM explanation as the gravitic field of the clusters.

Data Availability

The data underlying this article are available in the article and in its online supplementary material.

Conflicts of Interest

The author declares no conflicts of interest.

References

[1] Yang, Y., Ianjamasimanana, R., Hammer, F., Higgs, C., Namumba, B., Carignan, C., *et al.* (2022) Evidence of Ram-Pressure Stripping of WLM, a Dwarf Galaxy Far Away from Any Large Host Galaxy. *Astronomy & Astrophysics*, **660**, Article No. L11. https://doi.org/10.1051/0004-6361/202243307

[2] Kepley, A.A., Wilcots, E.M., Hunter, D.A. and Nordgren, T. (2007) A High-Resolution Study of the H I Content of Local Group Dwarf Irregular Galaxy WLM. *The Astronomical Journal*, **133**, Article No. 2242. https://doi.org/10.1086/513716

[3] Le Corre, S. (2015) Dark Matter, a New Proof of the Predictive Power of General Relativity. arXiv:1503.07440. (Preprint). https://arxiv.org/abs/1503.07440

[4] Hobson, M.P., Efstathiou, G.P., Lasenby, A.N., Hobson, M., Efstathiou, G. and Lasenby, A. (2009) Relativité générale. Cambridge University Press, Cambridge.

[5] Mashhoon, B. (2008) Gravitoelectromagnetism: A Brief Review. arXiv:0311030v2.

[6] Adler, R.J. (2015) The Three-Fold Theoretical Basis of the Gravity Probe B gyro

Precession Calculation. *Classical and Quantum Gravity*, **32**, Article ID: 224002. https://doi.org/10.1088/0264-9381/32/22/224002 https://iopscience.iop.org/article/10.1088/0264-9381/32/22/224002/meta

[7] Letelier, P.S. (2006) Rotation Curves, Dark Matter and General Relativity. *Proceedings of the International Astronomical Union*, **2**, 401-402. https://doi.org/10.1017/S1743921307005650

[8] Will, C.M. (2014) The Confrontation between General Relativity and Experiment. *Living Reviews in Relativity*, **17**, Article No. 4. arXiv:1403.7377v1. https://doi.org/10.12942/lrr-2014-4

[9] Bruni, M., Thomas, D.B. and Wands, D. (2013) Computing General Relativistic Effects from Newtonian N-Body Simulations: Frame Dragging in the Post-Friedmann Approach. *Physical Review D*, **89**, Article ID: 044010. arXiv:1306.1562v1. https://doi.org/10.1103/PhysRevD.89.044010

[10] Leaman, R., Cole, A.A., Venn, K.A., Tolstoy, E., Irwin, M.J., Szeifert, T., Skillman, E.D., *et al.* (2009) Stellar Metallicities and Kinematics in a Gas-rich Dwarf Galaxy: First Calcium Triplet Spectroscopy of Red Giant Branch Stars in WLM. *The Astrophysical Journal*, **699**, 1-14. https://doi.org/10.1088/0004-637X/699/1/1 https://iopscience.iop.org/article/10.1088/0004-637X/699/1/1

[11] Khademi, M., Yang, Y., Hammer, F. and Nasiri, S. (2021) Kinematical Asymmetry in the Dwarf Irregular Galaxy WLM and a Perturbed Halo Potential. *Astronomy & Astrophysics*, **654**, Article No. A7. https://doi.org/10.1051/0004-6361/202140336 https://www.aanda.org/articles/aa/full_html/2021/10/aa40336-21/aa40336-21.html

[12] Ibata, R.A., Lewis, G.F., Conn, A.R., Irwin, M.J., McConnachie, A.W., Chapman, S.C., Collins, M.L., *et al.* (2013) A Vast Thin Plane of Co-rotating Dwarf Galaxies Orbiting the Andromeda Galaxy. *Nature*, **493**, 62-65. https://doi.org/10.1038/nature11717 https://www.nature.com/articles/nature11717

[13] Pawlowski, M.S., Pflamm-Altenburg, J. and Kroupa, P. (2012) The VPOS: A Vast Polar Structure of Satellite Galaxies, Globular Clusters and Streams around the Milky Way. *Monthly Notices of the Royal Astronomical Society*, **423**, 1109-1126. https://doi.org/10.1111/j.1365-2966.2012.20937.x https://academic.oup.com/mnras/article/423/2/1109/960824

[14] Müller, O., Pawlowski, M.S., Jerjen, H. and Lelli, F. (2018) A Whirling Plane of Satellite Galaxies around Centaurus: A Challenges Cold Dark Matter Cosmology. *Science*, **359**, 534-537. https://doi.org/10.1126/science.aao1858

[15] Poggio, E., Drimmel, R., Andrae, R., Bailer-Jones, C.A.L., Fouesneau, M., Lattanzi, M.G., *et al.* (2020) Evidence of a Dynamically Evolving Galactic Warp. *Nature Astronomy*, **4**, 590-596. https://doi.org/10.1038/s41550-020-1017-3

[16] Cheng, X.L., Anguiano, B., Majewski, S.R., Hayes, C., Arras, P., Chiappini, C., *et al.* (2020) Exploring the Galactic Warp through Asymmetries in the Kinematics of the Galactic Disk. *The Astrophysical Journal*, **905**, Article No. 49 https://doi.org/10.3847/1538-4357/abc3c2 https://iopscience.iop.org/article/10.3847/1538-4357/abc3c2

[17] Chrobáková, Ž. and López-Corredoira, M. (2021) A Case against a Significant Detection of Precession in the Galactic Warp. *The Astrophysical Journal,* **912**, Article No. 130. https://doi.org/10.3847/1538-4357/abf356 https://iopscience.iop.org/article/10.3847/1538-4357/abf356

[18] Le Corre, S. (2015) Dark Energy, a New Proof of the Predictive Power of General Relativity. https://hal-ens-lyon.archives-ouvertes.fr/ensl-01122689

[19] Le Corre, S. (2020) Negative Gravitational Mass: An Ideal Solution for Cosmology. *Access Library Journal*, **7**, Article No. e6070. https://doi.org/10.4236/oalib.1106070

[20] Le Corre, S. (2021) Recent Cosmological Anisotropy Explained by Dark Energy as Universes of Negative Gravitational Mass. *Open Access Library Journal*, **8**, Article No. e7587. https://doi.org/10.4236/oalib.1107587